

A Microbolometer Airborne Calibrated Infrared Radiometer: The Ball Experimental Sea Surface Temperature (BESST) Radiometer

William J. Emery, William S. Good, William Tandy, M. Izaguirre, Peter Minnett

Abstract— A calibrated radiometer has been developed to enable the collection of accurate infrared measurements of sea surface temperature (SST) from unmanned aerial vehicles (UAVs). A key feature of this instrument is that in situ calibration is achieved with two built-in black bodies (BBs). The instrument is designed so that the 2D microbolometer array produces infrared images incremented as the aircraft travels, resulting in a well-calibrated strip of SST. Designed to be carried by medium class UAVs, the Ball Experimental SST (BESST) instrument has also been successfully flown on manned aircraft. A recent intercalibration of BESST was carried out at the University of Miami using their National Institute of Standards and Technology (NIST) traceable water-bath BB and a Fourier Transform interferometer, the Marine Atmospheric Emitted Radiance Interferometer (M-AERI). The characterization of the BESST instrument with the Miami BB demonstrates the linearity and precision of the response of the microbolometer-based radiometer. Coincident measurements of SST from a nearby pier clearly demonstrated the excellent performance of the BESST instrument with a mean SST equal to that of the M-AERI and an RMS of 0.14 K very close to the precision of 0.1 K. Cold calibration was not possible in Miami due to condensation, but a Ball BB was characterized relative to the Miami water-bath BB and calibrations were made in Boulder at lower temperatures than were possible in Miami. The BESST instrument's performance remained linear and the mean and RMS values did not change. UAV flights were conducted in summer/fall of 2013 over the Alaskan Arctic.

Index Terms—Microbolometer, Radiometer, Sea surface temperature, Thermal infrared

W.J. Emery is a professor at the University of Colorado, Boulder, CO 80309 USA. (e-mail: William.Emery@colorado.edu).

W.S. Good is a Senior Engineer at Ball Aerospace & Technologies in Boulder, CO 80301 USA. (e-mail: wgood@ball.com).

W.D. Tandy Jr. is a Senior Engineer at Ball Aerospace & Technologies in Boulder, CO 80301 USA. (e-mail: wtandy@ball.com).

M.A. Izaguirre is a Research Associate at the Rosenstiel School of Marine and Atmospheric Science, Miami, FL 33149 USA. (e-mail: mizaguirre@rsmas.miami.edu).

P.J. Minnett is Chair of Meteorology and Physical Oceanography at the Rosenstiel School of Marine and Atmospheric Science, Miami, FL 33149 USA. (e-mail: pminnett@rsmas.miami.edu).

I. INTRODUCTION

Satellite infrared instruments measure the emitted radiation from the skin layer of the ocean, which is related in a rather complex fashion to the subsurface temperatures measured by buoys and ships [1][2][3][4]. To further advance our understanding, it is important that we improve our ability to collect well-calibrated coincident measurements of skin SSTs. Collecting more accurate data at altitudes close to the sea surface will also be of benefit since there are fewer atmospheric error terms to consider. The data from these infrared instruments could then be used to validate infrared measurements from polar and geostationary orbiting satellites. Despite these potential benefits, these validation measurements can presently only be made from either research vessels or merchant ships. Unfortunately, these ships cannot collect a sample over an area as large as even a single 1 km pixel of one of the satellite sensors. In addition, the rather slow speed of ships means that it is not possible to rapidly collect continuous in-situ skin infrared emitted radiation from ships over time. The result is that the intervals between data sets are likely to be longer than the time scales of the processes that control the variability of skin SST.

An attractive alternative would be to fly an infrared radiometer on a plane or a UAV that could measure two-dimensional strip-maps of skin-emitted thermal radiation. Such a radiometer would have to be much smaller and lighter than those that make measurements from a ship, but they would still have to conform to the standard for making accurate SST measurements by having two BBs to provide a frequent two-temperature calibration of the sensed infrared radiation. To build such an instrument, Ball Aerospace designed BESST around a microbolometer as the sensor array, which both simplified the instrument and made it light and small in size. To provide the BB calibration, two small BBs were built and installed. Since the measurement of SST includes a component reflected off the sea surface from directly incoming thermal radiation from the atmosphere, the BESST instrument also makes a sky observation to correct for reflected sky infrared radiation in the derivation of the SST. Finally, to provide continuity across these measurements, BESST uses the same microbolometer for viewing the sea, the reflected sky radiation, and the two reference BBs.

These requirements dictated the size and shape of the BESST radiometer. Thus, the design includes a mirror that changes the view of the microbolometer between the view

ports and the BBs. The temperature of one BB is allowed to “float” with the ambient temperature while the second BB is heated to at least 12 K above the temperature of the ambient BB. These temperatures are continuously monitored and recorded from various locations on the BESST instrument. The small size of these reference BBs might have been a cause for concern, but the results section will show that this concern turned out to be unjustified. In order to use the same microbolometer for both target and calibration sensing, a small mirror on a shaft attached to a step-motor was installed which rotates for each calibration sequence. The initial sampling scheme was to collect three SST samples per second for 53 seconds and then perform a seven second calibration sequence. The calibration sequence requires a brief loss of data by the BESST.

The BESST instrument was taken to the University of Miami’s Rosenstiel School of Marine and Atmospheric Science (RSMAS) for characterization with the NIST traceable water-bath BB [5][6] and for a comparison with the M-AERI [4]. Against the NIST traceable BB, the BESST instrument was found to behave linearly and these measurements were used in subsequent comparisons to calibrate the BESST measurements. Measurements of SST from a nearby pier showed the BESST instrument to have a mean SST exactly the same as the M-AERI and a standard deviation of only 0.14 K, which was only slightly larger than the 0.1 K precision claimed for the microbolometer. These results are also confirmed by earlier laboratory and field calibration experiments made in Colorado [7]. This value of the standard deviation also includes contributions from the M-AERI measurements which are also estimated to be ~ 0.1 K.

II. INSTRUMENT DESIGN

The radiometer was conceived of as a “pushbroom” imaging radiometer that would produce strips of infrared data as the aircraft flew forward. A 324 X 256 pixel thermal imaging uncooled microbolometer could be equipped with filters (in the 8-12 μm range) that include the wavelength ranges primarily used for SST observations from satellites. The goal of this design would be to have calibrated SST measurements accurate to ± 0.1 K. This would be achieved by frequent calibration with two onboard BBs and with a correction for reflected sky radiation in the thermal infrared.

In its final configuration, the BESST radiometer’s FOV is 18 degrees, covering 200 pixels cross-track resulting in a swath width of about 1/3 of flight altitude above ground level. We do not use pixels on the edge of the detector array (due to optical distortion) taking only the center 200 pixels to optimize performance. Thus, the image resolution depends on the altitude of the aircraft that carries the BESST. For altitudes of about 600 m, the surface resolution is about 1 m with a swath width of 200 m. An airborne system with this spatial resolution is able to resolve the SST variability within the 1km pixels typical of space-borne infrared radiometers.

From the start, BESST was a modular design with a central cube to which target baffles, BBs, mirror motor, and microbolometer focal plane array (FPA) would be attached (Fig. 1). This design has evolved only slightly and the BESST

instrument now appears as in Fig. 2. This image includes a mounting bracket for a particular UAV.

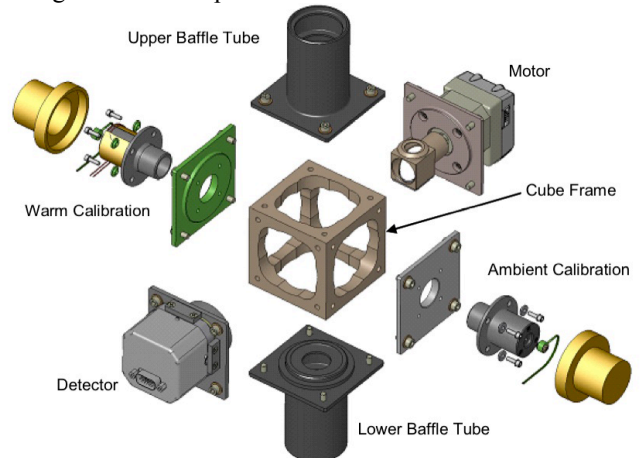


Figure 1. Modular design of the BESST radiometer

A single germanium lens looks through the downward looking baffle to collect incident radiation from the target scene, focusing it onto a two-dimensional uncooled microbolometer detector with a pixel size of 38 microns. The microbolometer is a FLIR Photon Thermal Imaging Camera Core (www.flir.com). The optical system is F/2 with a 25 mm focal length. The detector is partitioned into three spectral bands by the use of individual interference filters positioned in front of the detector array. The channels selected are fairly narrow channels centered at 10.8 μm and another centered at 12 μm . These channels are selected to correspond to the primary infrared channels used by satellite radiometers to compute SST. The third channel is broad, covering 8-12 μm , and provides a more sensitive SST channel by integrating a larger amount of thermal radiation. In processing, these channels can be treated individually or they can be combined to generate an SST product. The filters are placed along the flight path viewing the same ground scene with a latency of 0.3 s or less, depending on the platform’s speed over the ground. An anti-reflective coating on the germanium window into the focal plane array has a pass band from 8 to 12 μm and that provides additional out-of-band blocking into the microbolometer.

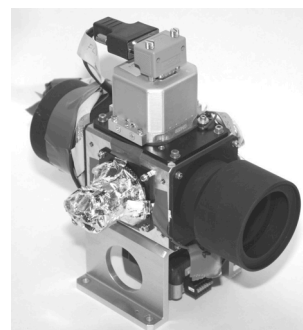


Figure 2. BESST #1 in operational configuration.

The basic design principle is to have the motor/scene – mirror opposite the detector array as shown in Fig. 3. The motor rotation axis is directly in-line with the center of the detector array. In this way, the optical path reflects off the fold mirror and can be directed by rotating the fold mirror. The optical path always reflects off the mirror so that the only difference to the detector is the actual scene. In addition, the optical stop is built into the turret, so the stop rotates with the mirror. Thermistors continually monitor the temperatures of these elements for correction in processing the microbolometer data.

Onboard calibration is done by alternating the observed ocean scene and the two temperature-monitored BB references, thus making it possible to construct a standard two-point calibration curve. A dark, uniform temperature flag (right above the filters and near the detector) provides a common reference for all pixels and is flipped in as part of the once per minute calibration routine.

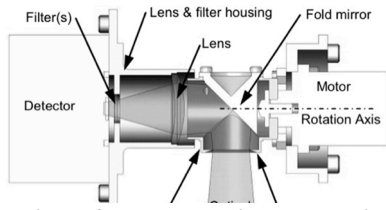


Figure 3. Detector, mirror and drive motor configuration

For calibration, the mechanical design has three distinct advantages. First, the tight fit between the mirror housing and the lens housing keeps stray light off of the calibration sources. Second, the angle of incidence of the mirror is equal for the calibration sources and the scene. Third, the area of the mirror is the same for both the calibration source and the target scene. The sky view is also part of the corrections to calculate SST in that it corrects for the sky radiation reflected into the downward looking radiometer.

A. Calibration Modules

The calibration targets consist of an aluminum tube with a conical end that forms the blackbody calibration source. The inside is painted with black absorptive paint so that when the detector views the BB it sees an accurately defined and uniform temperature. The calibration module shown in Fig. 4 can be made in two different configurations depending on the calibration temperature required. For a warm calibration source, a fiberglass-mounting flange is used so that the BB target is thermally isolated from the rest of the system. A strip heater, attached to the outside of the aluminum tube, heats the tube to a predetermined temperature (about 12 K above ambient) and the thermistor attached to the module reports its temperature. For the ambient module, no heater is installed and the temperature is monitored to insure that its temperature is close to the temperature of the sensor-mounting cube. The BBs and temperature sensors are covered by Mylar insulation to protect them from radiative heating and to trap the heat in the calibration module. The design of the BBs also protects them from contamination by rain while the insulation reflects sunlight.

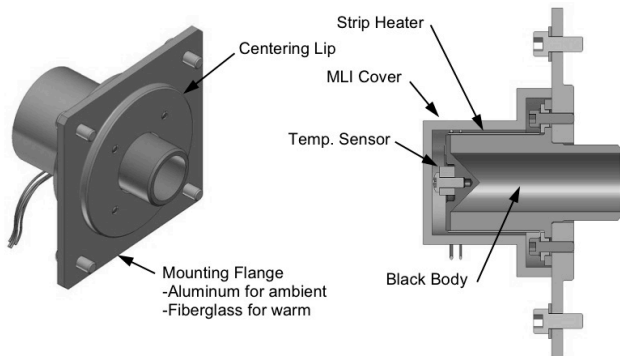


Figure 4. Calibration modules

B. Mass

The total mass of the BESST instrument is presented here in Table 1 and does not include the electrical cables, computer, or battery required to operate the system. The heaviest component on the list is the motor. The motor also includes a gear head and control electronics. A much simpler and lighter motor could be procured, but the selected unit proved adequate for the task as it was easy to interface with and easy to control. Even with this motor, the total weight is very light, making this an ideal instrument for flying on even rather small UAVs.

Table 1 Mass Summary

Module	Mass (grams)
Cube Frame	180
Motor	380
Detector	225
Baffle	110
Baffle	110
Cal Source	95
Cal Source	110
Mounting Bracket	150
Total	1.36 kg (3 lb)

The detector array captures images of each scene and the BB readings are used to provide highly accurate calibrations of the scene measurements. The sequence is automated by the

mini-PC software, which also collects the data over the region of interest. For this data collection, the frame rate is 3 Hz. A delay of 333 ms between frames and the inherent mini-PC computer latency makes this overall frame rate slightly less than 3 Hz. A total of 130 frames are collected during a data frame, which takes about 53 s and a calibration cycle takes just 7 s. Again, computer latency can affect these time periods, but time stamping of images with GPS time from a receiver allows accurate knowledge of image collection time.

C. Electronics

A block diagram of the BESST electronics is shown here in Fig. 5. The airborne computer is a dedicated mini-PC that controls the mirror position and records the data from the microbolometer. The motor is commanded to rotate the central fold mirror to view the four scenes: water, sky, warm BB, and ambient BB. The calibration cycle itself takes about 7 s resulting in about 21 frames of target data lost during a calibration cycle. Thus, for a 25 m/s ground speed of the UAV, BESST would collect data for 1.3 km and then undergo a calibration cycle for 0.2 km, which would then be repeated over the flight of the UAV.

Overall, the BESST instrument is collecting target data 87% of the time.

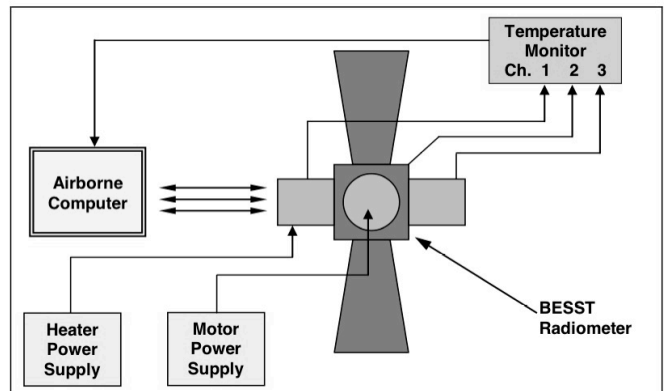


Figure 5. BESST electronics schematic

III. ABSOLUTE CALIBRATION

Initial laboratory calibrations at Ball with a reference BB indicated the absolute BESST accuracy to be ± 0.3 K. This reference BB was not NIST traceable, however, and this absolute accuracy is better than the repeat performance over the Great Salt Lake. To better establish the absolute temperature accuracy of the BESST, we carried out an intensive intercomparison experiment at the University of Miami’s Rosenstiel School of Marine and Atmospheric Science (RSMAS) in June of 2012. RSMAS has a NIST traceable BB to use as a reference and also operates the Marine-Atmosphere Emitted Radiance Interferometer (M-AERI) for SST measurements from ships. The plan for this intercomparison was to first characterize BESST against the RSMAS water-bath BB and then make an independent set of BB comparisons to test the absolute accuracy of the measurements made in the laboratory. Then both M-AERI and BESST would be taken to a nearby pier to make coincident measurements of SST over a period of time. This pier intercomparison was cut short due to the arrival of afternoon storms but the two instruments were operated coincidentally for at least 2 hours. In addition, lab measurements were made to characterize the Ball BB in terms of the Miami NIST traceable BB. This turned out to be a future advantage since condensation due to the humid Miami atmosphere restricted comparison with the NIST BB at lower temperatures where we hoped to operate BESST in the future. These reference measurements were later made back in Boulder with the Ball BB which had now been characterized against the Miami NIST traceable, water-bath BB as will be described below.

The characterization measurements of BESST against the Miami water-bath BB are presented here in Fig. 6. An average value of the reported temperatures within the area of the water-bath blackbody in the BESST 2-D image is plotted. The BESST raw temperature are found to be linear relative to the water-bath BB temperatures, indicating a predictable performance of the microbolometer when calibrated with its internal BBs. This intercomparison uses the best linear fit between the BESST onboard warm and cold BBs to interpolate the target bath temperature.

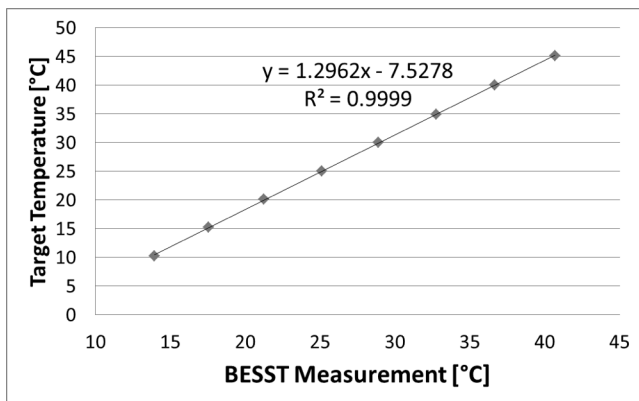


Figure 6. Comparison of NIST calibrated BB target temperatures to raw BESST measurements under ambient conditions

From the plot, we can determine the slope and offset for the line that corrects the measured BESST value to the actual target scene temperature. These constants can then be applied to correct future temperature measurements. When this is done with the same data set we used to derive the values, we get temperature errors that range between -0.1 and $+0.06$ K (within the ± 0.1 K precision of the microbolometer). Another independent data set was collected to estimate this scatter. The results are presented in Fig. 7.

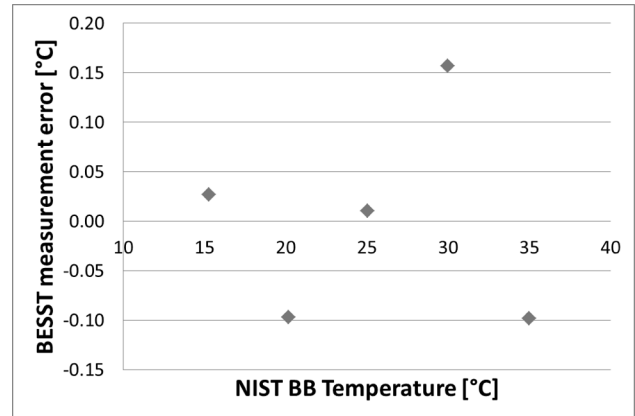


Figure 7. Independent measurement applying linear correction to raw BESST data

The scatter of this small data set ranges from 0.027 to $\pm 0.157^{\circ}\text{C}$. All of the differences are less than 0.16°C which is close to the absolute error of 0.1°C suggested by the earlier characterization measurements.

As mentioned previously, the characterization of the BESST instruments’ performance was not extended below 10°C for the Miami testing due to condensation on the NIST and Ball BB’s in the relatively humid atmosphere. In order to extend the range of calibrated performance of the instrument, BESST was installed in a dry nitrogen filled thermal chamber with the newly characterized Ball BB where the temperature could be lowered without condensation. The Ball BB was cross calibrated with the NIST BB during the Miami testing using the MAERI as a transfer radiometer. The resulting linear fit to the error of the Ball BB setpoint versus actual radiant temperature is shown in Fig 8. This slope and offset was applied to correct later data sets with the Ball BB making it possible to extend the BESST characterization to colder temperatures than were possible in the Miami characterization study.

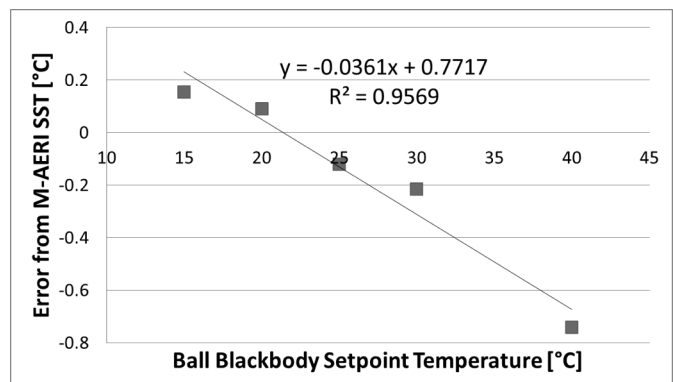


Figure 8. Linear fit to characterize Ball BB versus the NIST BB

Having calibrated the Ball BB versus the NIST traceable, water-bath Miami BB, measurements were collected under cold ambient conditions over a range of Ball BB target temperatures (Fig. 9). The measurements show linear performance of the BESST instrument for various ambient temperature conditions. Measurements of ambient temperature are collected by the thermistors mounted on the BESST internal ambient blackbody and on the instrument itself and updated for every data sample at 1.5 Hz. There is also another thermistor installed on the “hot” black body. The changing ambient temperature due to field conditions including altitude changes is used to determine the linear fit to apply to the BESST data in order to accurately find the target scene temperature for each image. A look up table of interpolated slopes and offsets provides the necessary correction for changing ambient temperatures. This ambient temperature correction is required due to non-linearities in the sensitivity of the microbolometer array to external temperature changes. The microbolometers are designed to operate nominally at 25°C and their sensitivity to incident thermal radiation varies when the temperature varies from this nominal condition. Time stamps synchronize the temperature data with the image data to allow for post-processing of all of the BESST data with the ambient temperature correction slopes and offsets.

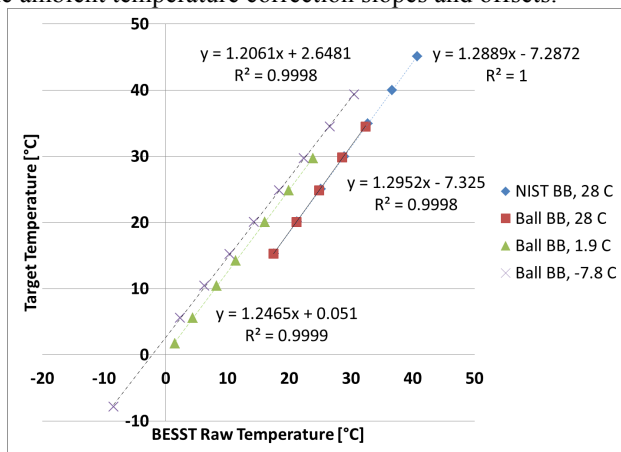


Figure 9. Characterization at varying ambient temperatures

Next, both the M-AERI and the BESST instruments were taken to a nearby pier to make coincident measurements of SST for an extended period. The BESST (Fig.10, top red dashed box) was mounted on top of the much larger M-AERI (bottom yellow dashed box) so as to approximately view the same water surface.



Figure 10. BESST (top-red) and M-AERI (bottom-yellow) mounted on pier

The view angle for the M-AERI is 55 ° and the height from the pier to the water surface was approximately 2 m. The M-AERI was about 0.61 m above the pier surface while BESST was about 1.22 m above the pier. M-AERI was viewing about

3.05 m away from the pier while BESST was nadir mounted and viewed the water about 0.46 m in front of the M-AERI aperture. The local current and the shallow (5 m) depth resulted in the observed surface waters being well mixed, which would result in a rather uniform SST. Two hours of coincident data were collected. The results are shown in Fig. 11, which is a time series plot of both the BESST and M-AERI measurements of the SST. For these measurements, a water emissivity of 0.9876 was used for the BESST 8-13 μm band where the characterization values in Fig. 9 were used to calibrate BESST for these measurements. An average of the temperatures from the central area of the BESST image is shown in the figure. The M-AERI values are averages of wavelengths near 7.7 μm [4]. As can be seen in Fig. 11, the BESST values showed a transient over the first 30 min of the time series. The M-AERI transient values dominated the entire first hour for some unknown reason (which may be due to a problem with the hot BB heater) and have been eliminated from this plot. While M-AERI has a measurement every ten minutes, the BESST instrument is putting out 3 measurements per second during these observations.

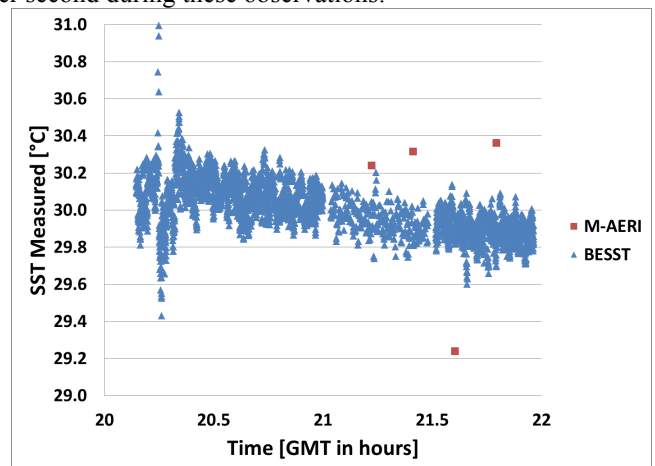


Figure 11. Sea surface temperature from Miami pier

Interestingly, both the BESST and the M-AERI recorded the same mean SST of 30.18 K over the entire two-hour period. The BESST measurements included the upward looking sky correction for reflected radiation and the M-AERI data were corrected for both reflected sky radiation and for atmospheric humidity. For the intercomparison, the first hour of M-AERI measurements were neglected and only the last four M-AERI SST measurements are included in Fig. 12. Over this shorter period, M-AERI gave a mean SST of 30.04 K while the BESST data for this period yielded a mean value of 30.01 K. The M-AERI SST standard deviation for this period was 0.54 K while that for the BESST was 0.14 K. The large variability for the M-AERI is clearly due largely to the single low value at about 21.7 hours. The BESST data also show a slight SST decrease at this point in time but do not go as low as the M-AERI value. Taken over the entire series, the SST standard deviation for BESST is only 0.14 K which includes the transient start-up period, which is consistent with the claimed 0.1 K precision of the microbolometer.

BESST measurements exhibit a relatively small variability and a nearly constant SST after about the point labeled as 21.5 hours on the plot. The time axis refers to Greenwich Mean

Time as collected by the instruments during the measurements.

IV. PAST AND FUTURE FIELD EXPERIMENTS

BESST was also flown on a Twin Otter aircraft over the Deepwater Horizon oil spill in the Gulf of Mexico in the summer of 2010 [8]. The goal of this deployment was to determine how well the BESST instrument would represent the oil slicks in conjunction with coincident measurements made by visible and radar instruments. Unfortunately, the radar did not operate properly and the visible instrument collected only a very limited data set. BESST, however, performed well and provided some very interesting images of the SST associated with surface oil. In Fig. 12 we present an image (left) of the SST along a BESST strip located over the oil as indicated by the map in the center panel collected along the track shown in the right panel. These data were collected during the day time when the oil is typically warmer than the surrounding water as is suggested by the red and yellow patches in the left panel of Fig. 12. The temperature range is 24-36°C. The

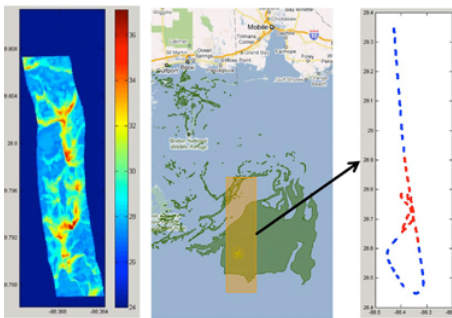


Figure 12. BESST SST example (left panel) collected along flight track (right panel).

The orange stripe corresponds to the flight path region blown up on the right panel and represents the location of the BESST SSTs collected. The loop represents the area where the plane turned around to go back on the same dashed line. The SST panel on the left is not completely rectangular reflecting the changes in plane location due to local winds. The interesting thing about the infrared sensing of oil is that, during the daytime, the oil appears warmer than the surrounding water while at night the oil cools faster than the water and an infrared image should then show the oil as cool relative to the water. The real benefit here is the rapid collection of this SST information and its ability to capture the fine detail that is not possible with satellite imagery.

The first UAV deployments were made in summer/fall of 2013 on the ScanEagle UAV which is a medium class UAV platform used frequently for video reconnaissance by the military.

The BESST instrument is integrated into a payload bay for this aircraft as shown here in Fig. 13.

The big advantage of operating an accurate SST radiometer from a small UAV is the ability of these aircraft to fly low and slow over the water for an extended period of time. Thus, they will operate below the major atmospheric attenuation layer and will be able to directly measure the complex spatial structure of the SST.

We will be able to actually measure the SST wavenumber spectrum of a 1 km² pixel of the typical infrared satellite SST



Figure 13. BESST in ScanEagle payload bay

sensor. This will help to resolve the long-standing question of how much sub-pixel spatial variability contributes to the uncertainty budget in the satellite SST retrievals when this is derived using comparisons with point measurements from buoys.

V. DISCUSSION AND CONCLUSIONS

The Ball Experimental Sea Surface Temperature (BESST) radiometer has been developed to be a small, accurate, compact and low-cost thermal infrared radiometer for UAV deployments. Both laboratory and field measurements have demonstrated that this instrument is capable of making SST measurements accurate to ± 0.14 °C with no bias difference and with accurate reference temperatures. Based on a microbolometer, the BESST instrument does not require cooling and its small size makes it possible to be deployed in even the smaller classes of UAVs. Laboratory measurements against a water-bath black body demonstrate the linear behavior of the BESST instrument. Coincident pier measurements with an interferometer (M-AERI) demonstrate the comparable behavior of the BESST instrument and recommend it as a small and low-cost alternative to measuring in situ skin SST. Alternative BESST designs were considered, but the upward and downward view ports are the most logical for UAV applications. In the future, a sea going version may be needed and the positions of the baffle tubes and the BBs may be changed. Such a sea-going instrument would also need rain and sea spray protection mechanisms. Fortunately, a primary advantage of the BESST's modular design is the flexibility to enable such alternative configurations.

VI. ACKNOWLEDGEMENTS

The authors would like to acknowledge the continued support of Ball Aerospace in developing BESST, funding the test flights and the Miami intercomparison tests. We would also like to acknowledge Michele Kuester, who began development of BESST back when she worked at Ball. We would like to acknowledge Erik Baldwin-Stevens who, as an intern at Ball, carried out a lot of the initial characterization of BESST. We also want to thank Robert Warden, Paul Kaptchen, and Tim Finch for their contributions to the development and testing of BESST. We also acknowledge NASA support of this instrument as part of MIZOPEX (<http://ccar.colorado.edu/mizopex/index.html>).

VII. REFERENCES

- [1] W.J. Emery, S. Castro, G.A. Wick, P. Schluessel and C. Donlon, "Estimating sea surface temperature from infrared satellite and in situ temperature data," *Bull Am. Meteor. Soc.*, 82, 2773 – 2785, 2001.
- [2] C.J. Merchant and A.R. Harris, "Toward the estimation of bias in satellite retrievals of sea surface temperature 2: Comparison with in situ measurements," *J. Geophys. Res.-Oceans*, 104, 23579-23590, 1999.

[3] C.J. Donlon, P. Minnett, C. L. Gentemann, I. J. Barton, B. Ward, J. Murray, and T. J. Nightingale, "Towards operational validation of satellite sea surface skin temperature measurements for climate research," *J. Climate*, 15(4), 353–369, 2002.

[4] P.J. Minnett, R. O. Knuteson, F.A. Best, B.J. Osborne, J. A. Hanafin, and O. B. Brown, "The Marine-Atmospheric Emitted Radiance Interferometer (M-AERI), a High-Accuracy, Sea-Going Infrared Spectroradiometer," *J. Atm Ocean Tech*, 18, no. 6, 994-1013, 2001.

[5] J.B. Fowler, "A Third Generation Water Bath Based Blackbody Source," *J. Res. of the National Institute of Standards and Technology*, 100, no. 5, 591-599, 1995.

[6] J.P. Rice, J. J. Butler, B. C. Johnson, P. J. Minnett, K. A. Maillet, T. J. Nightingale, S. J. Hook, A. Abtahi, C. J. Donlon, and I. J. Barton, "The Miami 2001 Infrared Radiometer Calibration and Intercomparison: 1. Laboratory Characterization of Blackbody Targets," *J. Atm Ocean Tech*, 21, 258-267, 2004.

[7] W. Good, R. Warden, P. Kaptchen, T. Finch and W. Emery, "Absolute thermal radiometry from a UAS," presented at the *AIAA Infotech@Aerospace Conference*, St. Louis, MO, 2011.

[8] W.S. Good, R. Warden, P.F. Kaptchen, T. Finch, W. J. Emery, and A. Giacomini, "Absolute Airborne Thermal SST Measurements and Satellite Data Analysis from the Deepwater Horizon Oil Spill," in *Monitoring and Modeling the Deepwater Horizon Oil Spill: A Record-Breaking Enterprise*, Geophysical Monograph Series 195, American Geophysical Union, 2011, 10.1029/2011GM001114.



William (Bill) Emery received his PhD in Physical Oceanography from the University of Hawaii in 1975. After working at Texas A&M University he moved to the University of British Columbia in 1978 where he created a Satellite Oceanography facility/education/research program. He was appointed professor in Aerospace Engineering Sciences at the University of Colorado, Boulder Campus in 1987. He is an Adjunct Professor of Informatics at Tor Vergata Univ in Rome, Italy. He has authored over 177-refereed publications on both ocean and land remote sensing and 2 textbooks. He is a fellow of the IEEE (2002) and the VP for publications of the IEEE Geoscience and Remote Sensing Society (GRSS). He received the GRSS Educational Award in 2004 and its Outstanding Service Award in 2009. He is a member of the IEEE Periodicals Committee. He is a Fellow of the American Meteorological Society (2010), the American Astronautical Society (2011) and the American Geophysical Union (2012).



William (Bill) S. Good received his M.S. degree in Aerospace Engineering Sciences from the University of Colorado in 2003. He achieved an M.S. degree in Condensed Matter Physics from Iowa State University in 2002. Mr. Good has worked at Ball Aerospace & Technologies since 2003 developing new instruments for Earth Remote

Sensing including UV-LWIR spectrometers and IR radiometers. Since 2008, Mr. Good has led the Ball Civil and Operational Space Airborne Initiative. He has been a member of the American Geophysical Union since 2009.



William (Bill) Tandy Jr. received his M.S. degree in Aerospace Engineering from the University of Texas at Austin in 2006. Mr. Tandy has worked at Ball Aerospace & Technologies since 2006 as a structural analyst as well as a systems engineer. Key projects include the JWST aft optics bench, the MOIRE spacecraft, and the OMPS ozone monitoring instrument. He has been involved with the BESST system as a programmer, developer, and operator since 2010.



Miguel Angel Izaguirre is a Research Associate at the Rosenstiel School of Marine and Atmospheric Science (<http://www.rsmas.miami.edu>) located at the University of Miami. Mr. Izaguirre has participated in numerous research cruises throughout the Atlantic, Pacific and Indian Oceans, the Caribbean Seas and the Gulf of Mexico, and many field campaigns in the Canary Islands, Barbados, Puerto Rico and the Maldives. His focus of interest is in Atmospheric Physics and Chemistry, and instrumentation.



Peter J Minnett, Member IEEE, has a BA in Physics from the University of Oxford in the UK, and MSc and PhD degrees in Oceanography from the University of Southampton, UK. Since 1995 he has been at the Rosenstiel School of Marine and Atmospheric Science of the University of Miami, Florida, where he is currently Chair of Meteorology and Physical Oceanography. His research interests lie in deriving accurate measurements of ocean variables, primarily sea-surface temperature, by remote sensing from satellites and ships. He serves as Science Team Chair of the Group for High Resolution Sea-Surface Temperature (GHRSSST).